TÜBİTAK

Turkish Journal of Earth Sciences

http://journals.tubitak.gov.tr/earth/

Research Article

Turkish J Earth Sci
(2013) 22: 671-680

doi:10.3906/yer-1205-3

Coastal inundation due to sea level rise and extreme sea state and its potential impacts: Çukurova Delta case*

Özlem SİMAV[1,], Dursun Zafer ŞEKER[2], Cem GAZİOĞLU[3]**

[1]General Command of Mapping, Tıp Fakültesi Caddesi, Dikimevi, Ankara, Turkey
[2]Faculty of Civil Engineering, İstanbul Technical University, Maslak, İstanbul, Turkey
[3]Institute of Marine Sciences and Management, İstanbul University, Vefa, İstanbul, Turkey

Received: 14.05.2012 • **Accepted:** 19.12.2012 • **Published Online:** 13.06.2013 • **Printed:** 12.07.2013

Abstract: With the rising sea level becoming a more pressing issue to coastal areas, a comprehensive analysis has been conducted to assess the vulnerability of the Çukurova Delta under the projected inundation by the end of the century. The level of inundation was estimated from a multimission satellite altimetry sea level anomaly and significant wave height data between September 1992 and February 2012. Superposed to the clear annual oscillation with 6.2 cm amplitude peaking around the beginning of October, the mean sea level signal exhibits a positive trend of 3.4 ± 0.1 mm/year over the altimetric data period. The extreme wave height with a 100-year return period is estimated to be about 6.1 ± 0.03 m, based on extreme probability distribution of the significant wave height data. In addition, taking the effects of tidal and meteorological forcings on the sea level into account, the maximum level of flooding expected to occur by the year 2100 reaches up to 6.7 m. GIS-based inundation mapping on the high resolution elevation model indicates that 69% of the area would be at risk of flooding. Nearshore settlements, lagoons, and the agricultural lands are the most severely impacted areas due to the inundation. The results can contribute to enhancing wetland conservation and management in the Çukurova Delta.

Key words: Coastal vulnerability, inundation, satellite altimetry, GIS, Çukurova Delta, Turkey

1. Introduction

Coastal zones, considered to be a valuable economic and environmental resource for human and marine habitats, are the most dynamic natural environment of any region on earth. Changes in the ocean–climate system and increasing human activities in these regions make the coastal areas more susceptible to natural hazards and more costly to live in. One of the most serious problems is the accelerated sea level rise and its resulting physical impacts on the coastal zones. Any rise in the mean sea level may result in the retreat of unprotected coastlines due to coastal inundation, erosion, and increased storm flooding (Nicholls *et al.* 1995). As emphasized in the Fourth Assessment Report of the Intergovernmental Panel on Climate Change (IPCC AR4), the global sea level rose by 1.8 to 3.1 mm/year during the last century and present estimates of future rise range from 18 cm to 59 cm by the year 2100 (Solomon *et al.* 2007). Low lying areas such as beach ridges, coastal plains, deltas, estuaries, lagoons, and bays would be the areas that would suffer the most as a result of the enhanced sea level rise. Thus, it is essential to quantify the response of coastal systems to sea level change, as well as to assess the potential threats posed to human and marine biodiversity.

A near global comparative analysis by Dasgupta *et al.* (2007) regarding the impact of permanent inundation due to sea level rise on 84 developing countries revealed that hundreds of millions of people in the developing world are likely to be displaced by a sea level rise of 1 to 5 m within this century. Accompanying economic and ecological damage will be severe for many. Approximately 0.3% (194,000 km^2) of the territory of the 84 developing countries would be impacted by a 1-m rise. This would increase to 1.2% in areas where the sea level rose 5 m. Nearly 56 million people (approximately 1.28% of the population) in these countries would be impacted under a 1-m rise scenario. This would increase to 89 million people for 2 m and 245 million people (approximately 5.57%) for a 5-m rise. The impact of sea level rise on gross domestic product (GDP) is slightly greater than the impact on population, because GDP per capita is generally above average for coastal populations and cities. Wetlands would experience significant impact even with a 1-m rise. Up to 7.3% of wetlands in the 84 countries would be impacted

* This manuscript solely reflects the personal views of the authors and does not necessarily represent the views, positions, strategies, or opinions of the Turkish Armed Forces.

** Correspondence: ozlem.simav@hgk.msb.gov.tr

by a 5-m sea level rise. However, these impacts are not uniformly distributed across the regions and countries of the developing world. Among the regions, East Asia and the Middle East/North Africa exhibit the greatest relative impacts. At the country level, the consequences of the sea level rise are potentially catastrophic in Vietnam, Egypt, and the Bahamas. For the land area, the Bahamas is by far the most impacted country. Close to 12% of its area would be affected by a 1-m rise. Around 10% of Vietnam and Egypt's populations, 10% of Vietnam's GDP and urban extent, 13% of Egypt's agricultural extent, and 28% of Vietnam, Jamaica, and Belize's wetlands would be impacted by the permanent inundation due to a 1-m sea level rise.

Surrounded by sea on 3 sides, Turkey could experience appreciable coastal impacts from sea level rise. Although coastal cities cover less than 5% of the country, at least 30 million people inhabit these places and the population is still growing at a rapid rate (Karaca & Nicholls 2008). Recent national and local scale investigations in Turkey have shown that some coastal areas, particularly the low lying deltaic plains, are highly vulnerable to the future sea level rise (Demirkesen *et al.* 2008; Karaca & Nicholls 2008; Alpar 2009; Kuleli *et al.* 2009; Kuleli 2010). The vulnerability of the Turkish coastal areas to permanent inundation was quantified by Demirkesen *et al.* (2008) based on the synthetic scenarios of constant sea level changes and the digital elevation model acquired by shuttle radar topography mission (SRTM). The analysis revealed inundated coastal areas of 545 to 2125 km^2 due to a sea level rise of 1 to 3 m, respectively. Coastal plains of the Seyhan and Ceyhan Rivers; Akyatan Lagoon; Göksü Delta along the Mediterranean Sea; Güllük, Dalaman, Didim, Selçuk, and Gediz Delta along the Aegean Sea; Dalyan Lake along the Marmara Sea; and the Terkos Lake and Kızılırmak Delta along the Black Sea were reported as the coastal areas of high risk. An analogous study was conducted by Karaca & Nicholls (2008). They defined 2 coastal risk zones according to their distance to the shoreline and their elevation, in which a 1-m rise in sea level would have important direct and indirect effects. The results of this study show that more than 0.5 million people would be affected at least indirectly by a 1-m sea level rise. They established a crude estimate of potential adaptation costs of US$20 billion to protect these people and capital values. More detailed site specific studies of different coastal regions of Turkey have been recommended using more detailed data to further understand the climate induced effects on the coastal environment.

In this paper, we focus on the vulnerability of the Çukurova Delta, considered to be one of the most susceptible areas in the county, under the projected inundation by the end of the century. The specific objectives of the current research are to determine areas at risk of projected inundation in the Çukurova deltaic region and to assess the impact of inundation from environmental, social, and economic aspects. Different from the previous studies, the projected inundation not only considers the permanent component caused by sea level rise, but also the temporary inundation due to extreme wave and meteorological conditions. The projected inundation level has been estimated from multimission satellite altimetry observations using statistical methods rather than adopting a deterministic rise scenario. The spread of the flooding in the inundation mapping is constrained by implementing a particular connectivity rule between the cells of the elevation model instead of using a simple bathtub or zero-side rule. A high resolution local elevation model extracted from 1/25K topographic maps is used rather than a global model for the better delineation of the extent of the inundation. Up to date site specific vector and thematic data are gathered for the assessment of the potential impacts.

2. Description of the study area

Çukurova Delta is located on the easternmost part of the Mediterranean Sea, between the metropolitan center of Mersin and the Gulf of İskenderun in southern Turkey (Figure 1). The delta is surrounded by the great Taurus mountain range that stretches from west to northeast, providing natural barriers to the cold airflow from inner zones to the south. Typical Mediterranean climate is dominant in the plain: mild and rainy winters, and relatively hot and dry summers. It is almost the largest and most fertile deltaic plain in the country, with more than 20,000 km^2 of catchment areas formed by the alluvial deposits of the Seyhan and Ceyhan rivers. There are 4 lagoons in the region, 2 of which, Akyatan and Yumurtalık, are designated as Wetlands of International Importance by the Ramsar Convention. The delta is known for the important biodiversity of flora and fauna, which lead to the specially protected area status. A majority of the delta is used for agricultural purposes: particularly cotton, citrus, soy, peanuts, and corn harvest. A number of beaches serve as the nesting places for endangered sea turtles. The area also acts as stopover for the migrating birds voyaging from Africa to Europe. There are 2 administrative districts within the study area, Karataş and Yumurtalık, with population densities of about 24–35 per km^2 respectively, according to the National Census of 2011. The region has a long coastline (approximately 110 km) and it is mostly the cottage tourism that serves the local and domestic residents from the surrounding areas. The coastline from Mersin to Karataş is mostly farmland. Karataş and Yumurtalık coasts are home to cottages with a bird conservatory residing between the 2 areas. The ports of Yumurtalık

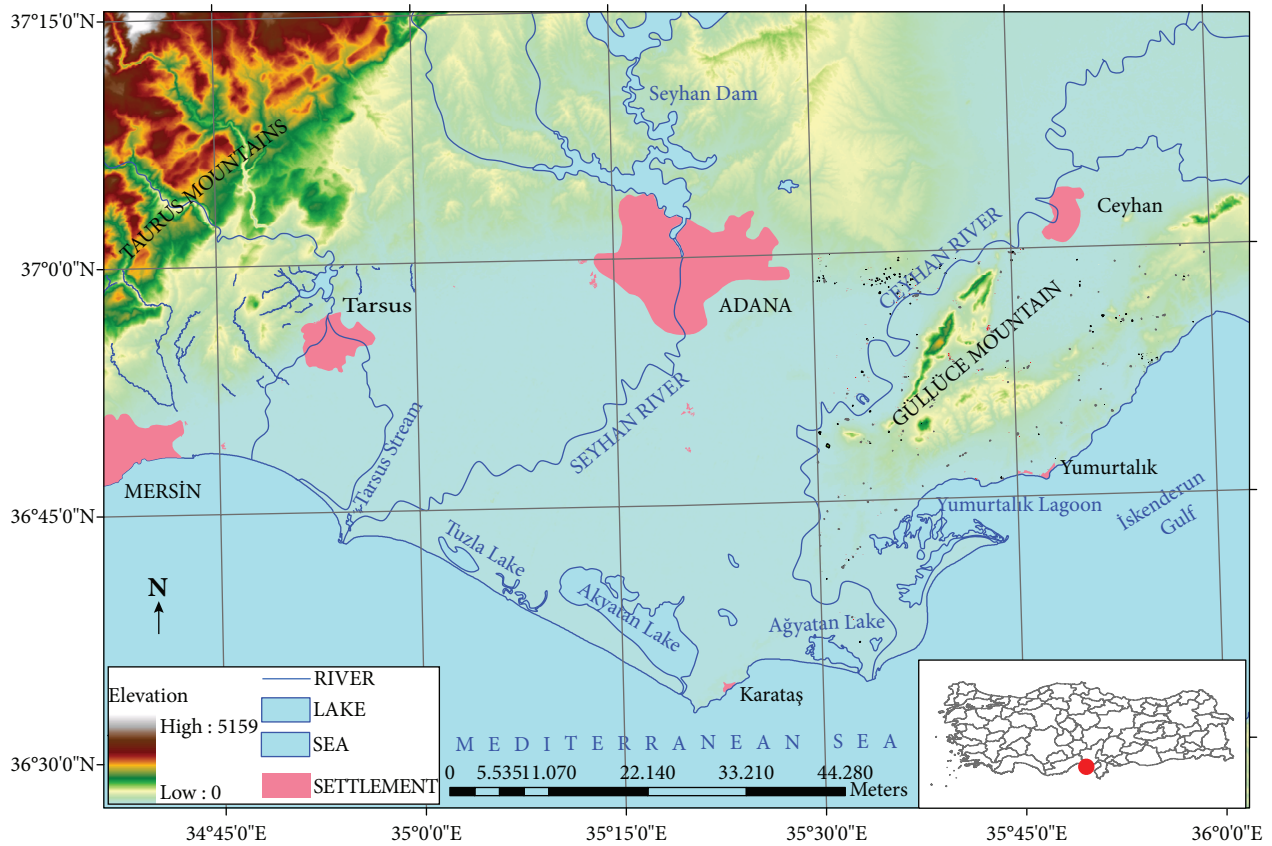

Figure 1. Study area (Çukurova deltaic region, Turkey).

and Ceyhan to the east are strategic locations for marine transportation, since the major East–West (Kirkuk–Yumurtalık) and North–South (Baku–Tbilisi–Ceyhan) route of crude oil pipelines terminates at these ports. All the physical, ecological, and socioeconomic properties of the delta demonstrate the value and importance of this low lying area. Thus, any rise in sea level will inevitably have adverse effects on the ecosystem of the delta on various levels.

3. Methodology

Several methods have been implemented in order to achieve the objectives of the research. The overall approach followed in this study is outlined in Figure 2. It involves the use of sea level and wave height data to estimate the inundation level, a digital elevation model to generate the coastal inundation map, satellite images to delineate agricultural land use, and other site specific information to superimpose on the inundation map in order to predict and assess the potential impacts of projected inundation.

3.1. Inundation modeling

In this study, the risk zone definition of Hoozemans *et al.* (1993) and Snoussi *et al.* (2008, 2009) has been adopted, where the inundation level (In_{Lev}) is given by the sum of mean high water (*MHW*), relative sea level rise (*S*), extreme wave height (H_{TR}), and sea level change due to the barometric pressure (S_p):

$$In_{Lev}=MHW+S+H_{TR}+S_P \quad (1)$$

Most of the quantities given in Eq. (1) have been computed from multimission satellite altimetry data. *MHW* is defined as the average of all the high water heights above the mean sea surface observed during the altimetry data period from 1992 to 2012. The highest sea level values over each satellite repeat cycle and pass within the study area are detected and averaged to estimate the *MHW* level relative to mean sea surface as follows:

$$MHW = \frac{1}{M}\sum_{i=1}^{m} max(SLA^{sat}_{cycle,\ pass}) \quad (2)$$

The current rate of sea level rise has been determined using a model including bias, trend, and seasonal terms that is given by:

$$SLA(t)=SLA(t_0)+A_1(t-t_0)+A_1cos(\omega_1 t-\varphi_1)+A_2cos(\omega_2 t-\varphi_2)+\varepsilon(t) \quad (3)$$

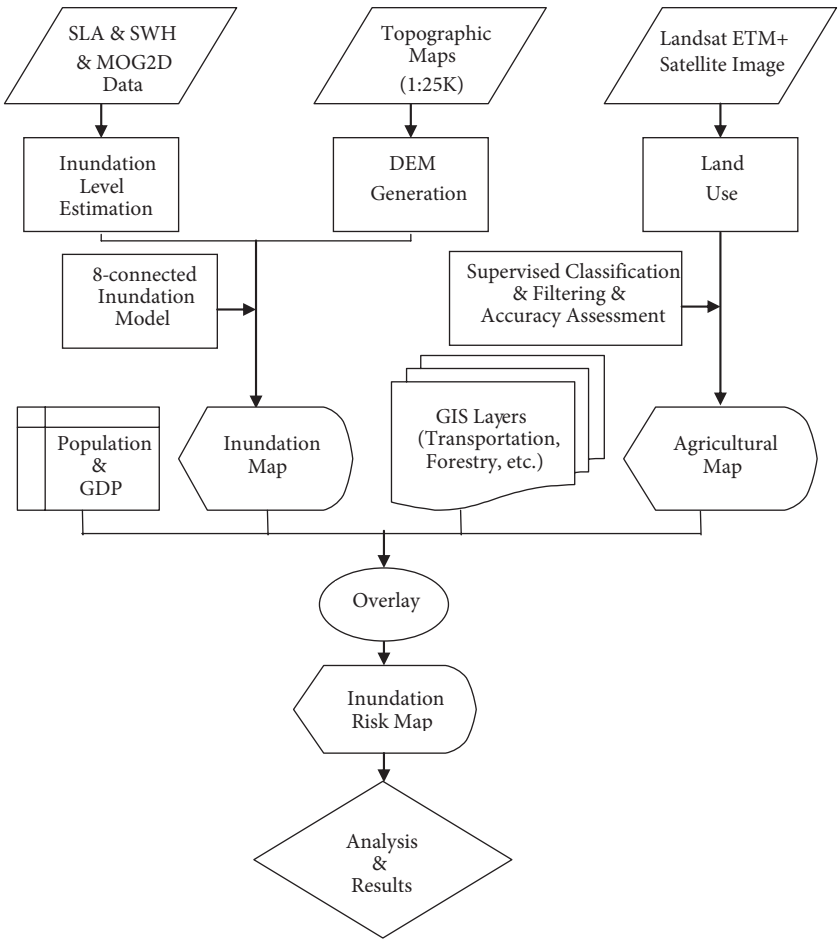

Figure 2. A schematic representation of the methodology used.

where t is time, t_0 is the origin of time or reference epoch, $SLA(t_0)$ is the initial sea level anomaly at time $t=t_0$, a_1 is a constant rate of sea level rise, and A_i, ω_i, φ_i are the amplitudes, angular frequencies, and phase angles of the annual (i=1) and semiannual (i=2) sea level signals, respectively. $\varepsilon(t)$ is the error term. The unknown parameters in Eq. (3) are derived by fitting the least squares regression to the altimetric sea level time series. Assuming there are no significant land movements (subsidence/uplift) in the vicinity of the study, no acceleration in the rate of sea level rise, and no interannual to decadal changes in the seasonal parameters, we have projected the relative sea level rise S by 2100 using the estimated parameters of the above harmonic model.

The extreme significant wave heights with T_R-year return values have been predicted using Gumbel extreme value distribution (Gumbel 1958; Kamphuis 2000; Suh 2007). According to this statistical distribution, the wave height expected for a selected return period H_R can be estimated as follows:

$$H_{TR}=\alpha-\beta In[In(1/P)] \quad (4)$$

where α and β represent the location and scale parameters, respectively, and P is the probability of nonexceedance. The model is fitted to the cumulative distribution function (CDF) of the altimetric wave data, which have been constructed using the following formula:

$$P = 1 - \frac{m}{N+1} \quad (5)$$

where m is the rank based on descending order of magnitude and N is the total number of passes or data points within the study area. The extreme wave height with a 100-year return period (H_{100}) has been predicted from the estimated parameters of the distribution model and the nonexceedance probability given by the formula below, where D is the decorrelation time scale in hours for significant wave height (SWH) observations (3 h), and T_{100} is the number of hours in 100 years (877,777.78 h, which includes leap years) (Suh 2007).

$$P(H < H_{100}) = 1 - \frac{D}{T_{100}} \quad (6)$$

Finally, the term S_p in Eq. (1) is computed from the MOG2D (2D Gravity Waves) model of Carrere & Lyard (2003). The model is used in the satellite altimetry data processing to account for the high frequency sea level variations caused by pressure and wind forcing. We consider the extreme meteorological contribution to sea level. Therefore, the term S_p is computed exactly in the same way as is done for *MHW*, where the highest values over each satellite repeat cycle and pass are averaged as follows:

$$S_P = \frac{1}{m}\sum_{i=1}^{m} max(MOG2D^{sat}_{cycle,\ pass}) \quad (7)$$

The "eight-side rule" approach proposed by Poulter & Halpin (2008) is used to simulate inundation in the study area rather than the simple bathtub or "zero-side rule". In this approach, a grid cell of the digital elevation model (DEM) is flooded only if its elevation is below the inundation level and if it is connected to an adjacent grid cell that is flooded or open water. Therefore, the surface connectivity between a grid cell and its immediate 8 neighbors in the cardinal and diagonal direction is taken into account. The rule can be expressed as follows:

$$F_{x,y} = \begin{cases} E_{x,y} \le In_{Lev}, 1 \\ E_{x,y} > In_{Lev}, 0 \end{cases} \mathrm{x}C \quad (8)$$

where F is binomial, either flooded (1) or not flooded (0); E is the elevation at location x,y; In_{Lev} is the projected inundation level; and C represents connectivity, either connected (1) or not connected (0).

3.2. Coastal topography and land use

Inundation mapping and analysis of flooding impacts require data on the land surface elevations, land use, and cover. We have produced a high resolution DEM for the study area from 1/25K topographic maps, instead of using freely available SRTM data. A triangular irregular network (TIN) has been constructed from the counter lines using the ArcGIS 3D Analyst tool that supports the Delaunay triangulation method. The generated TIN surface is then converted to a raster grid with regular cell spacing of 5 m using natural neighbor interpolation that implements an area based on a weighting scheme on the closest TIN nodes found in all directions around each output cell center (URL 1).

Agricultural land use within the study area is delineated from the Landsat-7 ETM+ satellite imagery acquired on 29 May 2006 (path/row-175/035) by means of image classification on the ERDAS platform. The satellite imagery, corrected and registered as GeoTIFF with 30-m resolution, is obtained from the Global Land Cover Facility website (URL 2). Supervised classification has been performed employing maximum likelihood classifier based on the training signatures established by onscreen digitizing of the false color composite image. The following 4 land use classes have been considered in image classification: agricultural land, wetland, forest, and bare ground. A fuzzy convolution filter with a window size of 7×7 is used to reduce the speckling of the classification before producing the final output. Overall map accuracy of 88.04% has been obtained based on 147 ground truth data interpreted from high resolution orthophoto maps, 1/25K topographic maps, and field knowledge. Finally, the classified image has been converted into vector format for further analysis.

4. Analysis and results

4.1. Satellite altimetry data and inundation level

The mean high water level, the rate of the mean sea level rise, and the extreme wave height with a return period of 100 years have been computed based on the sea level anomaly (SLA) and SWH data of Topex, Jason-1, Jason-2, Envisat, and Cryosat-2 altimeter satellites. The standard along-track altimetry data from the Radar Altimetry Data System (RADS) is extracted for the study area using version 3.1 of the default settings in the RADS database as described by Scharroo (2011). SLA and SWH time series cover Topex cycles 1 to 479 (September 1992 to September 2005), Jason-1 cycles 1 to 371 (January 2002 to February 2012), and Jason-2 cycles 0 to 133 (July 2008 to February 2012), each having average repeat cycles of 9.9 days. Envisat data span the time period from July 2002 to February 2012 (cycles 7 to 111), with an average repeat cycle of 35 days. We also use data delivered by satellite mission Cryosat-2 cycles 11 to 24 (February 2011 to January 2012). Figure 3 depicts the location of satellite ground tracks with different spatial resolutions. Along-track distance between 1-Hz measurements is about 7 km for most satellite missions, but the spacing between parallel tracks of Topex, Jason-1, and Jason-2 is about 300 km, and it is about 80 km for Envisat. Standard geophysical and environmental corrections including atmospheric, tidal, instrumental, and inverse barometer corrections have been applied to SLA data. Default data editing criteria (limits and flags) have been accepted during the SLA and SWH data construction. The sea level anomalies are given with respect to the DNSC08 global mean sea surface model derived from a combination of 12 years of satellite altimetry from 8 different satellites covering the period of 1993–2004 (Andersen & Knudsen 2009). During the inundation analysis, the mean surface is defined as the zero inundation level.

The 1-Hz SLA time series for an almost 20-year period covered by the satellite data is shown in Figure 4a. For the *MHW* level estimation, we first removed the tidal correction applied to the SLA data, then detected the

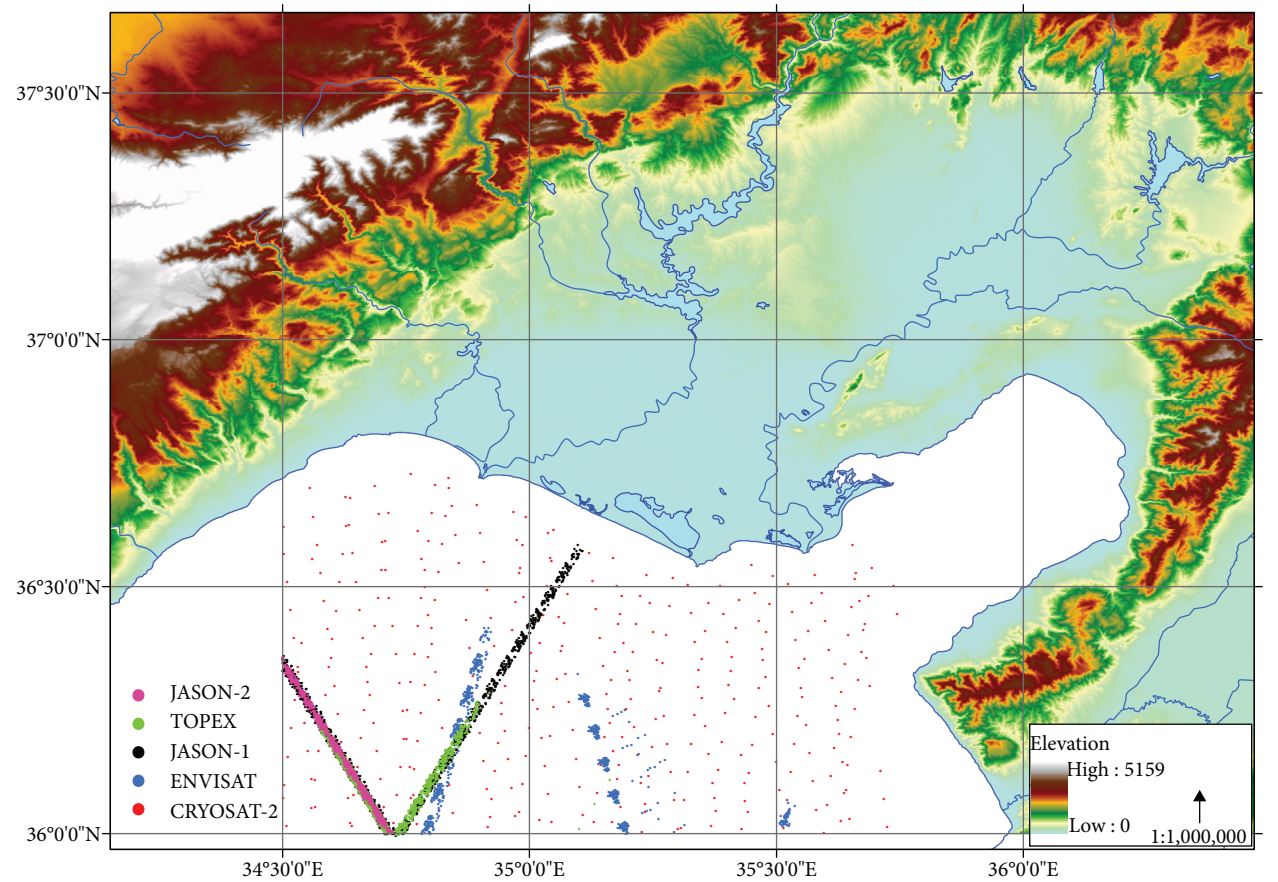

Figure 3. Topography of the study area in the landward side. Satellite altimetry data points (passes) in the seaward side (green: Topex, black: Jason-1, magenta: Jason-2, red: Cryosat-2, blue: Envisat satellite missions).

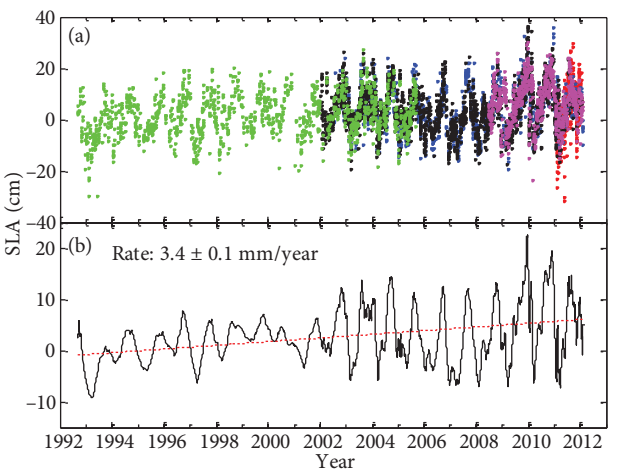

Figure 4. (a) 1-Hz multimission satellite altimetry sea level anomalies relative to DNSC08 mean sea surface between September 1992 and February 2012 (green: Topex, black: Jason-1, magenta: Jason-2, red: Cryosat-2, blue: Envisat satellite missions). (b) Smoothed mean sea level signal with a 60-day running filter (black line) and the rate of sea level rise (red dashed line).

highest values for each satellite repeat cycle and pass [see Eq. (2)]. After averaging these highest values, the height of *MHW* is found 19.5 cm above the DNSC08 mean sea surface.

The rate of sea level rise and seasonal variations are estimated from the mean sea level signal shown in Figure 4b, constructed by smoothing the multimission SLA data with a 60-day running mean filter (Cazenave *et al.* 2002; Willis *et al.* 2008). Note that the tidal correction is applied in this process. Table 1 shows the estimated parameters of Eq. (3) and the projected sea level rise by the year 2100 relative to the DNSC08 mean sea surface. A mean sea level rise of 3.4 ± 0.1 mm/year superimposed to the seasonal variations is apparent in Figure 4b that is quite consistent with the regional and global estimates (URL 3; Cazenave *et al.* 2008). Projection suggests that the mean sea level rises up to 35.8 ± 1.1 cm by the end of this century, which is also consistent with global mean sea level rise scenarios of IPCC AR4 (Solomon *et al.* 2007).

For the prediction of 100-year return wave height, we use SWH data from multimission satellite altimetry shown

Table 1. Estimated values and standard errors (one sigma) of the parameters in Eq. (3) and projected sea level rise by the year 2100.

$SLA(t_{2000})$ (cm)	α_1 (mm/year)	A_1 (cm)	φ_1 (degrees)	A_2 (cm)	φ_2 (degrees)	$SLA(t_{2100})$ (cm)
1.7 ± 0.1	3.4 ± 0.1	6.2 ± 0.1	269.9 ± 0.7	0.4 ± 0.1	41.8 ± 10.0	35.8 ± 1.1

in Figure 5a. For each satellite pass, we first compute the median of 1-Hz SWH data over each satellite repeat cycle. In the second step, these data are arranged in descending order and Eq. (5) is used to describe the empirical CDF, or probability, of nonexceedance of wave height. The SWH is then plotted against the reduced variate of Gumbel distribution $-In[In(1/P)]$ and a straight line is fitted to obtain the parameters of the probability distribution (Figures 5b and 5c). Using the nonexceedance probability of H_{100} [see Eq. (6)] and substituting the estimated parameters of probability distribution in Eq. (4), we have predicted the extreme wave height for a return period of 100 years. Table 2 gives the location and scale parameters of the Gumbel distribution, as well as the nonexceedance probability and predicted value of H_{100}.

In order to account for the mean meteorological forcing on the sea level, we have also downloaded the MOG2D total inverse barometer correction from the RADS database together with SLA and SWH data. Figure 6 shows the corresponding MOG2D corrections applied to 1-Hz SLA data in Figure 4a. The same methodology used in the *MHW* estimation is applied to the mean total inverse barometer signal. The highest values, depicted in Figure 6 with blue dots, for each satellite repeat cycle and pass are averaged [see Eq. (7)] to obtain the mean maximum meteorological forcing acting on the sea level (Figure 6, red line). Estimation of the mean sea level rises up to 4.7 cm as a result of extreme barometric conditions. Consequently, summing up the 4 contributors in Eq. (1), we obtain an inundation level of 6.7 m for the study area by the year 2100.

4.2. Inundation mapping and overlay analysis

The inundation model given in Eq. (8) has been evaluated in the ERDAS Imagine Virtual GIS Module using the projected inundation level of 6.7 m and the elevation model. The results of coastal vulnerability of the Çukurova Delta are summarized in Table 3, assuming no protection/adaptation measures are taken. The inundation map

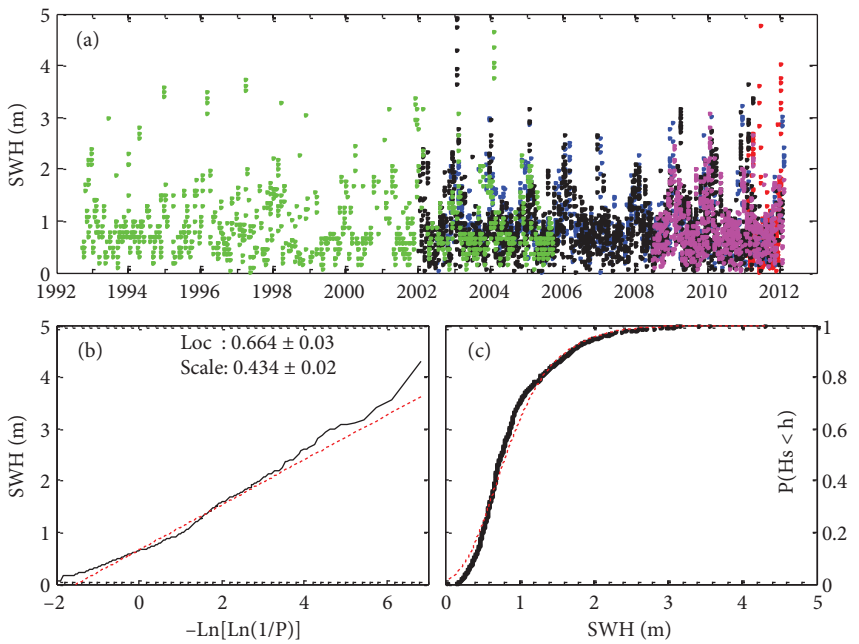

Figure 5. (a) The 1-Hz multimission satellite altimetry significant wave height data between September 1992 and February 2012 (green: Topex, black: Jason-1, magenta: Jason-2, red: Cryosat-2, blue: Envisat satellite missions). (b) Gumbel distribution plot (black line) and a straight line fit (red dashed line). (c) Cumulative distribution of the observed wave heights (black line) with its corresponding fit (red dashed line).

Table 2. Estimated values and standard errors (one sigma) of the parameters in Eq. (4), and nonexceedance probability and predicted value of extreme wave height for a 100-year return period.

α	β	$P(H < H_{100})$	H_{100} (m)
0.664 ± 0.003	0.434 ± 0.002	0.9999966	6.1 ± 0.03

presented in Figure 7 indicates that with the projected inundation of a given magnitude, about 69% of the total area would be at risk of flooding. Overlaying the inundated areas and land use map shows that about 68% of the agricultural areas, 100% of the wetlands, 77% of the settlement zones/beaches/bare lands, and 62% of the forestry lands would be exposed to permanent plus temporary inundation with the assumption that the land use pattern would remain the same as the current situation. The lagoons, nearshore settlements, and agricultural areas are the most vulnerable zones. Assuming a mean population density of 30 people per km^2 within the region and assuming zero-growth population in the future years, more than 42,000 people would be suffering from the inundation. The average GDP per capita is $2339 in the city of Adana, Turkey, and therefore at least $98,000,000 of the GDP would be affected. The extent of the inundation also affects the transportation, where almost 33% of the roadways would subject to flooding.

5. Conclusion and suggestions

Understanding the mechanisms of the sea level change and its impacts on the coastal ecosystem has gained increasing importance in the age of climate change. The projection of future sea level rise and resulting coastal inundation is a crucial task in order to raise the awareness of people, to set up efficient coastal management programs, and to mitigate probable hazard risks. This study focuses on the projected inundation of the Çukurova Delta, one of the most productive, but at the same time most susceptible to sea level rise, areas in Turkey. Multimission satellite altimeter data suggest that the inundation level within the region reaches up to 6.7 m by the year 2100. However, one should bear in mind that this magnitude comprises both the permanent and temporary components of the inundation, which approximately corresponds to the maximum level of flooding and does not reflect the duration of the inundation. With the projected inundation of this magnitude, about 69% of the area would be at risk of flooding, where the nearshore settlements, lagoons, and agricultural lands seem to be the most severely impacted areas.

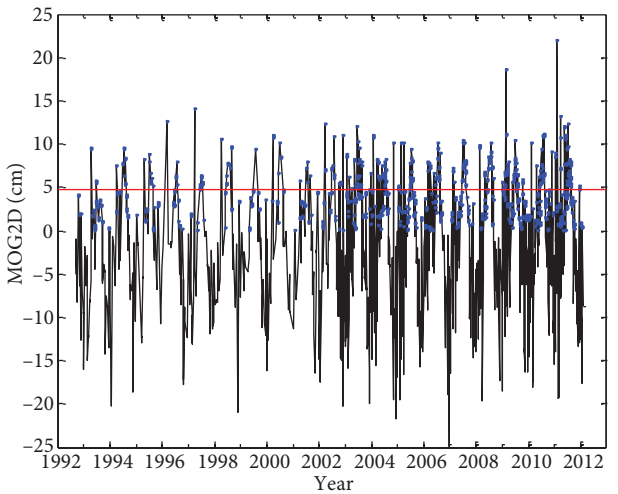

Figure 6. MOG2D time series for the sea level anomaly data in Figure 4a used to account for the high frequency sea level variations caused by pressure and wind forcing. Blue dots represent the highest values in each satellite repeat cycle and pass. Horizontal red line represents the mean of highest values.

This analysis is important to emphasize to what extent coastal protection and accommodation strategies might be necessary when considering sea level rise and storm flood scenarios. Even more detailed information is needed to precisely determine the full range of risks, and some further studies should be conducted to investigate the other physical impacts of sea level rise such as erosion and saltwater intrusion. Many national and international programs and projects have been initiated during the last few years, including the "Climate Change Adaptation in the Seyhan River Basin Grants Programme" (URL 4) and "Strong Civil Society Sustainable Çukurova River Basin Project" (URL 5), for the investigation of the vulnerability of the region and mitigation of the negative impacts of climate change. Even if the output of this study gives a preliminary estimation of the areas at risk, it may contribute to enhancing wetland conservation and management in the delta.

Despite some novelties brought by the use of satellite altimetry products in inundation level estimation of the study region for the first time, this study contains some limitations. Altimetric measurements are contaminated potentially by the signals from land and islands within their footprints. The tides are much more complex near the shores than in the open ocean and require a precise knowledge of the coastal geography of the study area. The wet tropospheric corrections computed from radiometer

Table 3. Results of the vulnerability assessment.

Indicator	Areas/length/unit	Affected part	Rate
Agricultural land	1397 km^2	952 km^2	68%
Wetland	41 km^2	41 km^2	100%
Forestry land	66 km^2	41 km^2	62%
Settlement, beach, bare land	399 km^2	309 km^2	77%
Total land	2035 km^2	1412 km^2	69%
Transportation (roads)	12,481 km	4163 km	33%
Population	30 people/km^2	42,360 people	
GDP	$2339/capita	$98,656,440	

measurements are also less precise or not present at all near the coasts. Using postprocessed coastal altimetry products or terrestrial data (e.g., tide gauge, wave buoy) may improve the estimations.

Satellite altimetry measures the absolute sea level variations, but we must be concerned about the relative sea level, or the observed change in water level relative to the level of the nearby land, when we deal with the inundation analysis. Any subsidence in the vicinity of the shoreline may raise the relative sea level or vice versa. In this study, we assume that there is no significant land movement (subsidence/uplift) in the vicinity of the study region, and thus absolute sea level from satellite altimetry is equivalent to relative sea level. We suggest that the vertical land movements should be monitored by independent techniques, such as Global Positioning System (GPS) or Interferometric Synthetic Aperture Radar (InSAR), and be taken into account in the estimation of inundation level.

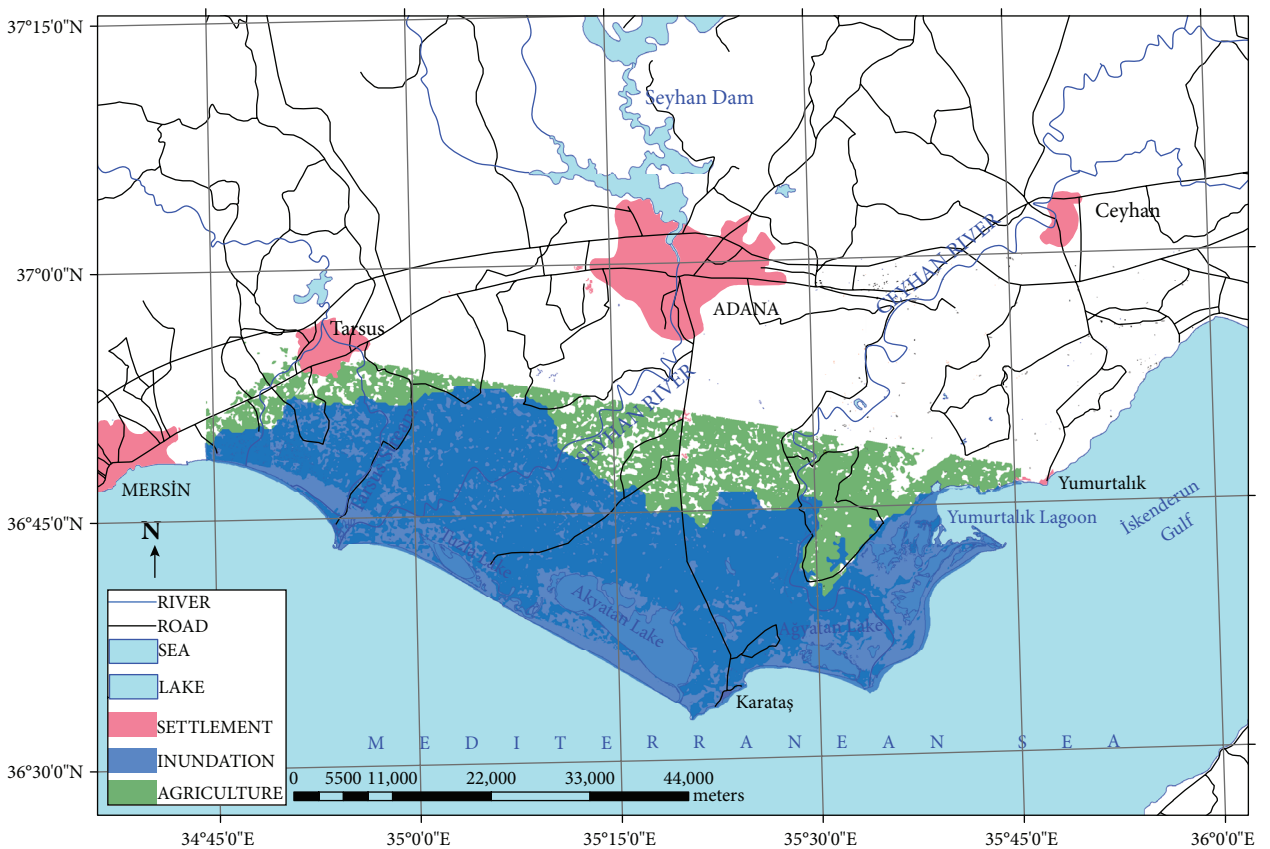

Figure 7. Projected inundation map of Çukurova Delta with a maximum inundation level of 6.7 m by the year 2100.

The digital elevation model is the primary dataset in inundation mapping. Using a high resolution and more accurate model will necessarily improve the results. In our study, we used a local elevation model extracted from topographic maps rather than a global model for the better delineation of the extent of the inundation. Terrestrial measurements by GPS or electronic tachometers, or by light detection and ranging (LiDAR) systems, will contribute to refining the model.

Acknowledgments
The authors wish to thank the following institutions that provided data: 1/25K topographic maps, elevation, transportation, forestry, and settlement GIS layers in vector formats were provided by the General Command of Mapping (Turkey); population and GDP data were from the Turkish Statistical Institute; Landsat-7 ETM+ satellite imagery was obtained from the Global Land Cover Facility website at www.glcf.umiacs.umd.edu; and satellite altimetry sea level anomaly, significant wave height, and MOG2D data were from the Radar Altimeter Database System at http://rads.tudelft.nl/rads/rads.shtml.

References

Alpar, B. 2009. Vulnerability of Turkish coasts to accelerated sea-level rise. *Geomorphology* **107**, 58–63.

Andersen, O.B. & Knudsen, P. 2009. DNSC08 mean sea surface and mean dynamic topography models. *Journal of Geophysical Research* **114**, C11001.

Carrere, L. & Lyard, F. 2003. Modeling the barotropic response of the global ocean to atmospheric wind and pressure forcing - comparisons with observations. *Geophysical Research Letters* **30(6)**, 1275.

Cazenave, A., Bonnefond, P., Mercier, F., Dominh, K. & Toumazou, V. 2002. Sea level variations in the Mediterranean Sea and Black Sea from satellite altimetry and tide gauges. *Global and Planetary Change* **34**, 59–86.

Cazenave, A., Dominh, K., Guinehut, S., Berthier, E., Llovel, W., Ramillien, G., Ablain, M. & Larnicol, G. 2008. Sea level budget over 2003–2008: A reevaluation from GRACE space gravimetry, satellite altimetry and Argo. *Global and Planetary Change* **65**, 83–88.

Dasgupta, S., Laplante, B., Meisner, C., Wheeler, D. & Yan, J. 2007. *The impact of sea level rise on developing countries: A comparative analysis*. World Bank Policy Research Working Paper, 4136. Available at http://econ.worldbank.org.

Demirkesen, A.C., Evrendilek, F. & Berberoğlu, S. 2008. Quantifying coastal inundation vulnerability of Turkey to sea-level rise. *Environmental Monitoring and Assessment* **138(1–3)**, 101–106.

Gumbel, E.J. 1958. *Statistics of Extremes*. Columbia University Press, New York.

Hoozemans, F.M.J., Marchand, M. & Pennekamp, H.A. 1993. *Sea Level Rise: A Global Vulnerability Assessment-Vulnerability Assessments for Population, Coastal Wetlands and Rice Production on a Global Scale*. 2nd ed. Delft Hydraulics, Delft, the Netherlands.

Kamphuis, J.W. 2000. *Introduction to Coastal Engineering and Management*. World Scientific, Singapore.

Karaca, M. & Nicholls, R.J. 2008. Potential implications of accelerated sea-level rise for Turkey. *Journal of Coastal Research* **24(2)**, 288–298.

Kuleli, T. 2010. City-based risk assessment of sea level rise using topographic and census data for the Turkish coastal zone. *Estuaries and Coasts* **33**, 640–651.

Kuleli, T., Şenkal, O. & Erdem, M. 2009. National assessment of sea level rise using topographic and census data for Turkish coastal zone. *Environmental Monitoring and Assessment* **156**, 425–434.

Nicholls, R.J., Leatherman, S.P., Dennis, K.C. & Volonte, C.R. 1995. Impacts and responses to sea-level rise: qualitative and quantitative assessments. *Journal of Coastal Research* **14**, 26–43.

Poulter, B. & Halpin, P.N. 2008. Raster modelling of coastal flooding from sea-level rise. *International Journal of Geographical Information Science* **22(2)**, 167–182.

Scharroo, R. 2011. *RADS User Manual and Format Specification (Version 3.1)*. Available at http://rads.tudelft.nl/rads/radsmanual.pdf.

Snoussi, M., Ouchani, T., Khouakhi, A. & Niang-Diop, I. 2009. Impacts of sea-level rise on the Moroccan coastal zone: quantifying coastal erosion and flooding in the Tangier Bay. *Geomorphology* **107**, 32–40.

Snoussi, M., Ouchani, T. & Niazi, S. 2008. Vulnerability assessment of the impact of sea-level rise and flooding on the Moroccan coast: the case of the Mediterranean eastern zone. *Estuarine Coastal and Shelf Science* **77**, 206–213.

Solomon, S., Qin, D., Manning, M., Chen, Z., Marquis, M., Averyt, K.B., Tignor, M. & Miller, H.L. 2007. *Climate Change 2007: The Physical Science Basis*. Contribution of Working Group I to the Fourth Assessment Report of the Intergovernmental Panel on Climate Change. Cambridge University Press, Cambridge, UK.

Suh, I.H. 2007. *Statistics of Amplitude and Fluid Velocity of Large and Rare Waves in the Ocean*. MSc Thesis, Department of Mechanical Engineering, Massachusetts Institute of Technology, USA.

Willis, J.K., Chambers, D.P. & Nerem, R.S. 2008. Assessing the globally averaged sea level budget on seasonal to interannual timescales. *Journal of Geophysical Research* **113**, C06015.

URL 1: http://webhelp.esri.com/arcgiSDEsktop/9.3/index.cfm?TopicName, 07.11.2012. Welcome to ArcGIS Desktop Help 9.3, including 9.3.1.

URL 2: www.glcf.umiacs.umd.edu, 07.11.2012. Global Land Cover Facility.

URL 3: http://www.aviso.oceanobs.com/en/applications/ocean/mean-sea-level-greenhouse-effect/regional-trends/index.html, 07.11.2012. AVISO.

URL 4: http://www.kad.org.tr/cukurova-deltasi, 07.11.2012. Kuş Araştırmaları Derneği Seyhan İklim Değişikliği Uyum Projesi.

URL 6: http://www.cukurovadeltasi.org/index.html, 07.11.2012. Çukurova Deltası.